5

Biped Gait Generation and Control Based on Mechanical Energy Constraint

Fumihiko Asano[1], Masaki Yamakita[2,1], Norihiro Kamamichi[1] &
Zhi-Wei Luo[3,1]
1. *Bio-Mimetic Control Research Center, RIKEN*
2. *Tokyo Institute of Technology*
3. *Kobe University*

1. Introduction

Realization of natural and energy-efficient dynamic walking has come to be one of the main subjects in the research area of robotic biped locomotion. Recently, many approaches considering the efficiency of gait have been proposed and McGeer's passive dynamic walking (McGeer, 1990) has been attracted as a clue to elucidate the mechanism of efficient dynamic walking. Passive dynamic walkers can walk down a gentle slope without any external actuation. Although the robot's mechanical energy is dissipated by heel-strike at the stance-leg exchange instant, the gravity potential automatically restores it during the single-support phase in the case of passive dynamic walking on a slope and thus the dynamic walking is continued. If we regard the passive dynamic walking as an active one on a level, it is found that the robot is propelled by the small gravity in the walking direction and the mechanical energy is monotonically restored by the virtual control inputs representing the small gravity effect. Restoration of the mechanical energy dissipated by heel-strike is a necessary condition common to dynamic gait generations from the mathematical point of view, and efficient active dynamic walking should be realized by reproducing this mechanism on a level. Mechanical systems satisfy a relation between the control inputs and the mechanical energy, the power-input for the system is equal to the time-derivative of mechanical energy, and we introduce a constraint condition so that the time-change rate of mechanical energy is kept positive constant. The dynamic gait generation is then specified by a simple redundant equation including the control inputs as the indeterminate variables and yields a problem of how to solve the equation in real-time. The ankle and the hip joint torques are determined according to the phases of cycle based on the pre-planned priority. The zero moment point (Vukobuatović & Stepanenko, 1972) can be easily manipulated by adjusting the ankle-joint torque, and the hip-joint torque in this case is secondly determined to satisfy the desired energy constraint condition with the pre-determined ankle-joint torque. Several solutions considering the zero moment point condition are proposed, and it is shown that a stable dynamic gait is easily generated without using any pre-designed desired trajectories. The typical gait is analyzed by numerical simulations, and an experimental case study using a simple machine is performed to show the validity of the proposed method.

Source: Humanoid Robots, New Developments, Book edited by: Armando Carlos de Pina Filho
ISBN 978-3-902613-02-8, pp.582, I-Tech, Vienna, Austria, June 2007

2. Compass-like Biped Robot

In this chapter, a simplest planar 2-link full-actuated walking model, so-called *compass-like walker* (Goswami *et al.*, 1996), is chosen as the control object. Fig. 1 (left) shows the experimental walking machine and closed up of its foot which was designed as a nearly ideal compass-like biped model. This robot has three DC motors with encoders in the hip block to reduce the weight of the legs. The ankle joints are driven by the motors via timing belts. Table lists the values of the robot parameters. Fig. 1 (right) shows the simplest ideal compass-like biped model of the experimental machine, where m_H , m [kg] and $l = a + b$ [m] are the hip mass, leg mass and leg length, respectively. Its dynamic equation during the single-support phase is given by

$$\boldsymbol{M}(\boldsymbol{\theta})\ddot{\boldsymbol{\theta}} + \boldsymbol{C}(\boldsymbol{\theta},\dot{\boldsymbol{\theta}})\dot{\boldsymbol{\theta}} + \boldsymbol{g}(\boldsymbol{\theta}) = \boldsymbol{\tau}\,, \tag{1}$$

where $\boldsymbol{\theta} = \begin{bmatrix}\theta_1 & \theta_2\end{bmatrix}^{\mathrm{T}}$ is the angle vector of the robot's configuration, and the details of the matrices are as follows:

$$\begin{aligned}
\boldsymbol{M}(\boldsymbol{\theta}) &= \begin{bmatrix} m_H l^2 + ma^2 + ml^2 & -mbl\cos(\theta_1 - \theta_2) \\ -mbl\cos(\theta_1 - \theta_2) & mb^2 \end{bmatrix}, \\
\boldsymbol{C}(\boldsymbol{\theta},\dot{\boldsymbol{\theta}}) &= \begin{bmatrix} 0 & -mbl\sin(\theta_1 - \theta_2)\dot{\theta}_2 \\ mbl\sin(\theta_1 - \theta_2)\dot{\theta}_1 & 0 \end{bmatrix}, \\
\boldsymbol{g}(\boldsymbol{\theta}) &= \begin{bmatrix} -(m_H l + ma + ml)\sin\theta_1 \\ mb\sin\theta_2 \end{bmatrix} g,
\end{aligned} \tag{2}$$

and the control torque input vector has the form of

$$\boldsymbol{\tau} = \boldsymbol{S}\boldsymbol{u} = \begin{bmatrix} 1 & 1 \\ 0 & -1 \end{bmatrix}\begin{bmatrix} u_1 \\ u_2 \end{bmatrix}. \tag{3}$$

The transition is assumed to be inelastic and without slipping. With the assumption and based on the law of conservation of angular momentum, we can derive the following compact equation between the pre-impact and post-impact angular velocities

$$\boldsymbol{Q}^{+}(\alpha)\dot{\boldsymbol{\theta}}^{+} = \boldsymbol{Q}^{-}(\alpha)\dot{\boldsymbol{\theta}}^{-}\,, \tag{4}$$

where

$$\begin{aligned}
\boldsymbol{Q}^{+}(\alpha) &= \begin{bmatrix} m_H l^2 + ma^2 + ml\left(l - b\cos(2\alpha)\right) & mb\left(b - l\cos(2\alpha)\right) \\ -mbl\cos(2\alpha) & mb^2 \end{bmatrix}, \\
\boldsymbol{Q}^{-}(\alpha) &= \begin{bmatrix} \left(m_H l^2 + 2mal\right)\cos(2\alpha) - mab & -mab \\ -mab & 0 \end{bmatrix},
\end{aligned} \tag{5}$$

and α [rad] is the half inter-leg angle at the heel-strike instant given by

$$\alpha = \frac{\dot{\theta}_1^{-} - \dot{\theta}_2^{-}}{2} = \frac{\dot{\theta}_2^{+} - \dot{\theta}_1^{+}}{2} > 0\,. \tag{6}$$

For further details of derivation, the authors should refer to the technical report by Goswami *et al.* This simplest walking model can walk down a gentle slope with suitable choices of physical parameters and initial condition. Goswami *et al.* discovered that this model exhibits period-doubling bifurcations and chaotic motion (Goswami *et al.*, 1996) when the slope angle increases. The nonlinear dynamics of passive walkers are very attractive but its mechanism has not been clarified yet.

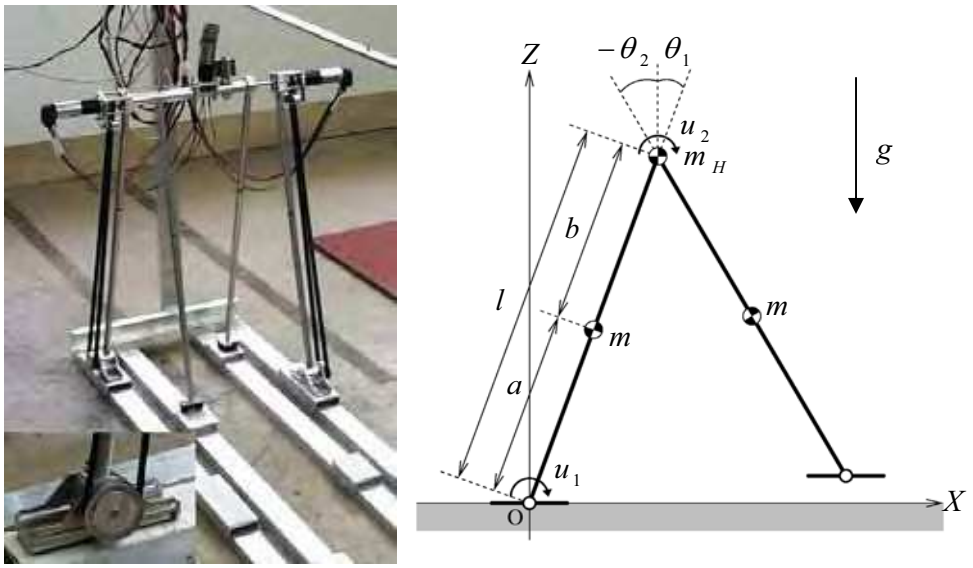

Fig. 1. Experimental walking machine and its foot mechanism (left), and its ideal model (right).

m_H		3.0	kg
m		0.4	kg
l	$=a+b$	0.680	m
a		0.215	m
b		0.465	m

Table 1. Physical parameters of the experimental machine.

3. Passive Dynamic Walking Mechanism Revisited

Passive dynamic walking has been considered as a clue to elucidate to clarify the essence of efficient dynamic walking, and the authors believe that it is worth investigating the automatic gait generation mechanism. The impulsive transition feature, non double-support phase, can be intuitively regarded as *vigor* for high-speed and energy-efficient walking. In order to get the *vigor*, the walking machine must restore the mechanical energy efficiently during the single-support phase, and the impulsive and inelastic collision with the ground dissipates it discontinuously. In the following, we describe it in detail.

The passive dynamic walker on a gentle slope can be considered to walk actively on a *virtual* level ground whose gravity is $g\cos\phi$ as shown in Fig. 2. The left robot in the figure is propelled forward by the small gravity element of $g\sin\phi$, and the right one walks by equivalent transformed torques. By representing this mechanism in the level walking, energy-efficient dynamic bipedal gait should be generated. The authors proposed virtual gravity concept for the level walking and called it "virtual passive dynamic walking." (Asano & Yamakita, 2001) The equivalent torques u_1 and u_2 are given by transforming the effect of the horizontal gravity element $g\sin\phi$ as shown in Fig. 2 left.

Let us define virtual total mechanical energy E_ϕ under the gravity condition of Fig. 2 as follows:

$$_\phi(\theta,\dot{\theta},\phi)_= \frac{1}{2}\dot{\theta}\ M(\theta)\dot{\theta} \quad P(\theta,\phi) \tag{7}$$

where the *virtual* potential energy is given by

$$P(\boldsymbol{\theta},\phi) = \left\{\left(m_H l + ma + ml\right)\cos\left(\theta_1 - \phi\right) - mb\cos\left(\theta_2 - \phi\right)\right\} g\cos\phi \cdot \tag{8}$$

In the case of passive dynamic walking on a slope, the total mechanical energy is kept constant during the single-support phase, whereas E_ϕ does not exhibit such behaviour. Fig. 3 shows the simulation results of passive dynamic walking on a gentle slope whose magnitude is 0.01 [rad]. (c) and (d) show the evolutions of the equivalent transformed torques and virtual energy E_ϕ, respectively. From (c), we can see that both u_1 and u_2 are almost *constant-like* and thus the ZMP should be kept within a narrow range. This property is effective in the virtual passive dynamic walking from the viewpoint of the stability of foot posture (Asano & Yamakita, 2001). It is apparent from (d) that the mechanical energy is dissipated at the transition instant and monotonically restored during the swing phase. Such energy behaviour can be considered as an indicator of efficient dynamic walking.

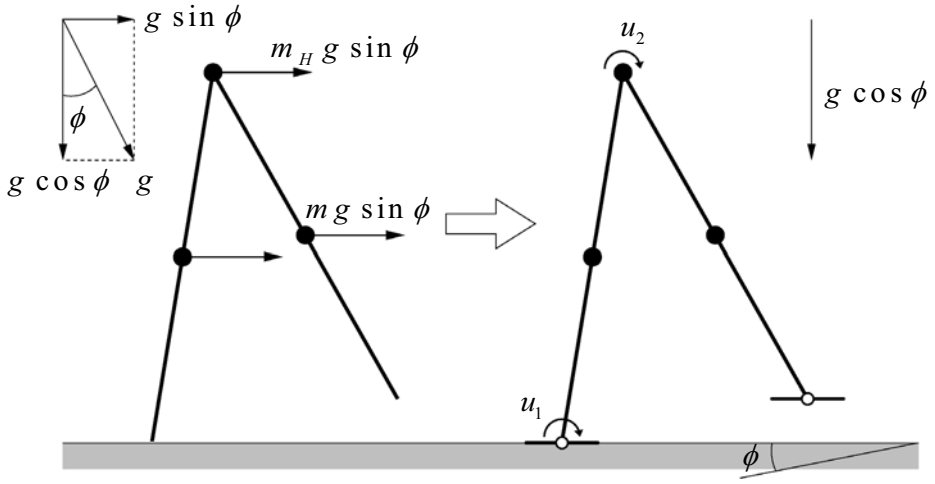

Fig. 2. Gravity acceleration mechanism of passive dynamic walking.

In general, we can state the following.

CH1) The total mechanical energy of the robot E_ϕ increases monotonically during the swing phase.

CH2) $\dot{\theta}_1 > 0$ always holds.

CH3) There exists an instant when $\theta_1 - \theta_2 = 0$.

CH1 and CH2 always hold, regardless of physical and initial conditions, but CH3 does not always hold, as it depends on physical parameters and slope angle. We can confirm CH2 and CH3 from Fig. 3 (a) and (b). It is also clear that CH1 holds from Fig. 3 (d). From the results, the essence of a passive dynamic gait should be summarized as follows.

E1) The walking pattern is generated automatically, including impulsive transitions, and converges to a steady limit cycle.
E2) The total mechanical energy is restored during the single-support phase monotonically, and is dissipated at every transition instant impulsively by heel-strike with the floor.
E2 is considered to be an important characteristic for dynamic gait generation, and is the basic concept of our method. We will propose a simple method imitating the property in the next section.

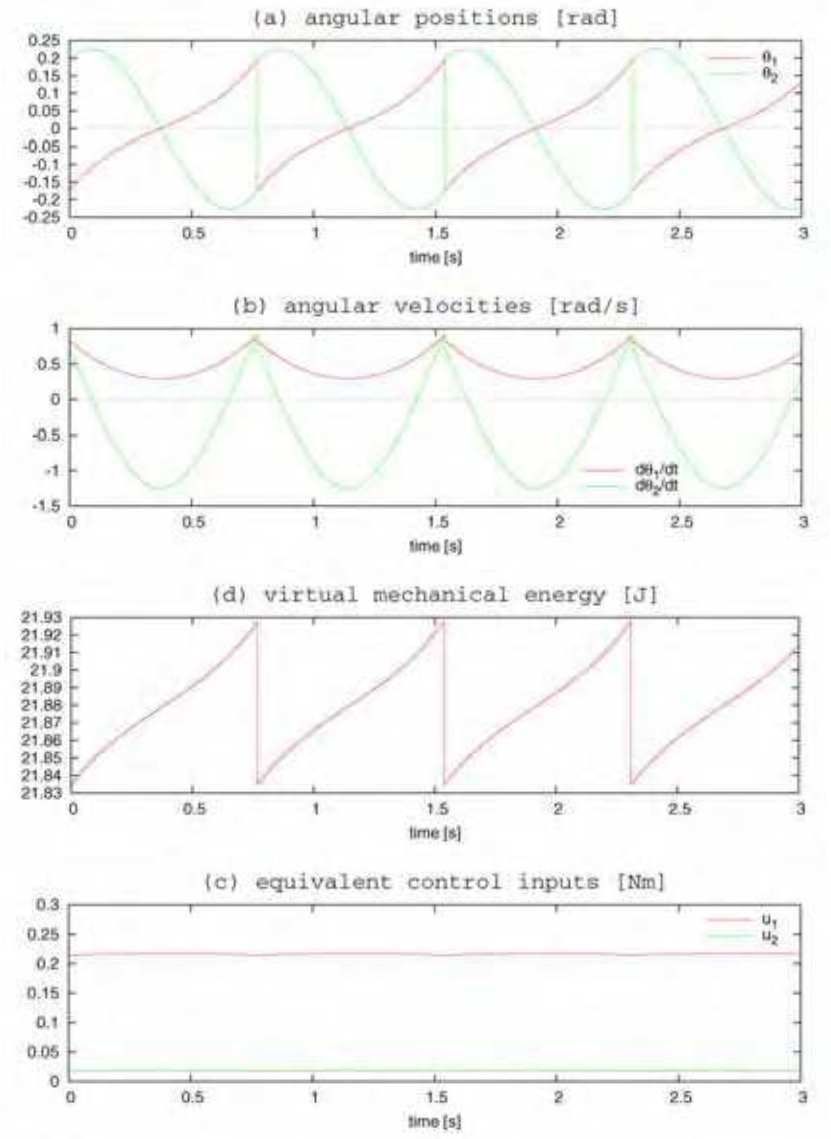

Fig. 3. Simulation results of passive dynamic walking on a slope where $\phi = 0.01$ [rad].

4.Energy Constraint Control

In our previous works, we have proposed virtual passive walking considering an artificial gravity condition called virtual gravity (Asano & Yamakita, 2001). This imitates the gravity acceleration mechanism of the original passive dynamic walking. A virtual gravity in the walking direction acts as a driving force for the robot and the stable limit cycle can be generated automatically without any gait design in advance. Determining a virtual gravity is, however, equivalent to that of control inputs, so there is no freedom to control other factors, for example, ZMP control. By imitating the property of monotonic energy restoration, however, we can formulate a simple method with a freedom of the control inputs.

4.1 The Control Law

The total mechanical energy of the robot can be expressed as

$$E\left(\boldsymbol{\theta},\dot{\boldsymbol{\theta}}\right)=\frac{1}{2}\dot{\boldsymbol{\theta}}^{\mathrm{T}}\boldsymbol{M}(\boldsymbol{\theta})\dot{\boldsymbol{\theta}}+P(\boldsymbol{\theta}), \tag{9}$$

where P is the potential energy. The power input to the system is the time-change rate of the total energy, that is

$$\dot{E}=\dot{\boldsymbol{\theta}}^{\mathrm{T}}\boldsymbol{\tau}=\dot{\boldsymbol{\theta}}^{\mathrm{T}}\boldsymbol{S}\boldsymbol{u}. \tag{10}$$

Suppose now that we use a simple control law imitating the characteristic CH1, monotonic energy restoration. Let $\lambda>0$ be a positive constant and consider the following condition:

$$\dot{E}=\lambda. \tag{11}$$

This means that the robot's mechanical energy increases monotonically with a constant rate of λ. We call this control or gait generation method "Energy Constraint Control (ECC)". In this method, the walking speed becomes faster w.r.t. the increase of λ, in other words, the magnitude of λ corresponds to the slope angle of virtual passive dynamic walking. Here let us consider the following output function:

$$H\left(\boldsymbol{\tau}\right)=\dot{E}-\lambda=\dot{\boldsymbol{\theta}}^{\mathrm{T}}\boldsymbol{\tau}-\lambda, \tag{12}$$

and the target constraint condition of Eq. (11) can be rewritten as $H\left(\boldsymbol{\tau}\right)=0$. Therefore, the ECC can be regarded in this sense as an output zeroing control.

Following Eqs. (10) and (11), the detailed target energy constraint condition is expressed as

$$\dot{E}=\dot{\boldsymbol{\theta}}^{\mathrm{T}}\boldsymbol{S}\boldsymbol{u}=\dot{\theta}_{1}u_{1}+\left(\dot{\theta}_{1}-\dot{\theta}_{2}\right)u_{2}=\lambda, \tag{13}$$

which is a redundant equation on the control inputs. The dynamic gait generation then yields a problem of how to solve the redundant equation for the control inputs u_1 and u_2 in real-time. The property of ECC strategy is that the control inputs can be easily determined by adjusting the feed-forward parameter λ, which can be determined by considering the magnitude of $\dot{E}$ of virtual passive dynamic walking.

4.2 Relation between ZMP and Reaction Moment

The actual walking machine has feet and a problem of reaction moment then arises. The geometrical specifications of the stance leg and its foot are shown in Fig. 4. In this chapter, the ZMP is calculated by the following approach. We assume:

1. The mass and volume of the feet can be ignored.
2. The sole always fits with the floor.

Under these assumptions, we can calculate the ZMP in the coordinate shown in Fig. 4 left as:

$$\text{ZMP} = -\frac{u_1}{R_n} \tag{14}$$

where u_1 [Nm] is the ankle torque acting not on the foot link but on the leg link and R_n [N] is the vertical element of the reaction force, respectively.

From Fig. 4, it is obvious that the ZMP is always shifted behind the ankle joint when driving the stance-leg forward, however, at the transition instant, the robot is critically affected by the reaction moment from the floor as shown in Fig. 4 right. Considering the reaction moment effect, we can reform the ZMP equation for the simplest model as follows:

$$\text{ZMP} = -\frac{u_1 + u_{\text{rm}}}{R_n} \tag{15}$$

where $u_{\text{rm}} > 0$ represents the equivalent torque of the reaction moment, and the ZMP is shifted backward furthermore. u_{rm} acts as a disturbance for the transition. Since the actual walking machines generally have feet with toe and heel, this problem arises. From the aforementioned point of view, we conclude that the ZMP should be shifted forward the ankle-joint just after the transition instant to cancel the reaction moment. Based on the observation, in the following, we consider an intuitive ZMP manipulation algorithm utilizing the freedom of the redundant equation of (13).

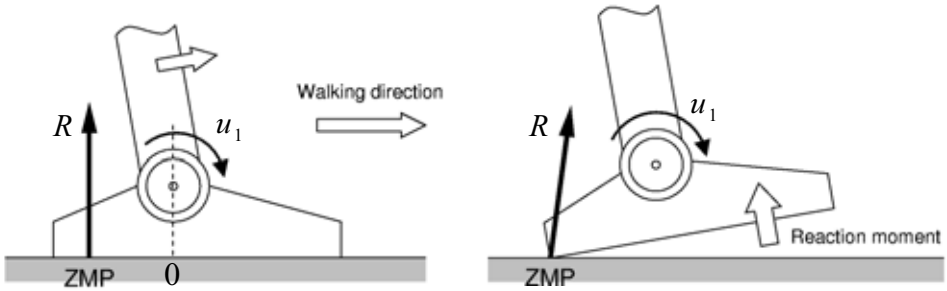

Fig. 4. Foot mechanism and reaction moment at the heel-strike instant.

4.3 Principal Ankle-joint Torque Control

From a practical point of view, as mentioned above, the two most important control factors of dynamic bipedal walking are mechanical energy restoration and ZMP control. To keep the energy constraint condition of Eq. (11), we should reconsider the solution algorithm.
Firstly, we should consider mechanical energy restoration to generate a gait, and secondly, ZMP condition must be guaranteed without destroying the constraint condition. Based on the considerations, we first discuss the following solution approach:

1. Determine the value of λ.
2. Determine the ankle torque u_1.
3. By substituting λ and u_1 into Eq. (13), we can solve it for u_2.

In order to shift the ZMP, let us consider the following simple ankle-joint torque control:

$$u_1 = \begin{cases} u^- < 0 & s \le T \\ u^+ > 0 & \text{otherwise} \end{cases} \tag{16}$$

where s is a virtual time that is reset at every transition instant and $\dot{s} = 1.0$. This comes from the fact that u_1 must be negative to shift the ZMP forward the ankle-joint, and if $u_1 > 0$ the ZMP moves behind the ankle-joint. In this case, u_2 is obtained after u_1 as follows:

$$u_2 = \frac{\lambda - \dot{\theta}_1 u^{\pm}}{\dot{\theta}_1 - \dot{\theta}_2}. \tag{17}$$

Note that u_2 has a singularity at $\dot{\theta}_1 - \dot{\theta}_2 = 0$ which was mentioned before as CH3. This condition must be taken into account. We then propose a switching control law described later. Before it, we consider a more reasonable switching algorithm from u^- to u^+. In general, for most part of a cycle from the beginning, the condition $\dot{\theta}_1 - \dot{\theta}_2 > 0$ holds (See Fig. 3 (b)), and thus the sign of u_2 of Eq. (17) is identical with that of $\lambda - \dot{\theta}_1 u_1$. If $u_1 = u^-$, this sign is positive because of $\lambda, \dot{\theta}_1 > 0$ and $u^- < 0$. At the beginning of a cycle, $\lambda - \dot{\theta}_1 u^+$ increases monotonically because of $\ddot{\theta}_1 < 0$ (See Fig. 3 (b)). Therefore in general the condition

$$\frac{\mathrm{d}}{\mathrm{d}t}\left(\lambda - \dot{\theta}_1 u^+\right) = -\ddot{\theta}_1 u^+ > 0 \tag{18}$$

holds regardless of the system parameter choice. Therefore, if $\lambda < \dot{\theta}_1 u^+$ at the beginning, it is reasonable to switch when

$$\lambda - \dot{\theta}_1 u^+ = 0 \tag{19}$$

so as to keep u_2 of Eq. (17) always positive under the condition of $\dot{\theta}_1 - \dot{\theta}_2 > 0$. In addition, by this approach the hip-joint torque can always contribute the mechanical energy restoration. The switching algorithm of u_1 is summarized as follows:

$$u_1 = \begin{cases} u^- < 0 & \lambda \le \dot{\theta}_1 u^+ \\ u^+ > 0 & \text{otherwise} \end{cases}. \tag{20}$$

The value of u^+ must be determined empirically based on the simulation results of virtual passive dynamic walking, whereas u^- should be determined carefully so as not to destroy the original limit cycle or disturb the forward acceleration. Choosing the suitable combination between λ and u^+ is the most important for generating a stable limit cycle.

4.4 Principal Hip-joint Torque Control

As mentioned before, we must switch the controller to avoid the singularity of CH3 at the end of the single-support phase. As a new method, we propose the following new strategy:

1. Determine the value of λ.
2. Determine the hip torque u_2.
3. By substituting λ and u_2 into Eq. (13), we can solve it for u_1.

In this case, u_1 is determined by the following formula:

$$u_1 = \frac{\lambda - \left(\dot{\theta}_1 - \dot{\theta}_2\right) u_2}{\dot{\theta}_1}. \tag{21}$$

Note that here we use the assumption of CH2. In this paper, as a reasonable candidate of u_2, we consider the following form:

$$u_2 = \eta\left(\dot{\theta}_1 - \dot{\theta}_2\right). \tag{22}$$

Assuming $\eta > 0$, this leads the following inequality:

$$\left(\dot{\theta}_1 - \dot{\theta}_2\right) u_2 = \eta\left(\dot{\theta}_1 - \dot{\theta}_2\right)^2 \geq 0, \tag{23}$$

therefore it is found that this hip-joint torque u_2 also contributes the mechanical energy restoration.

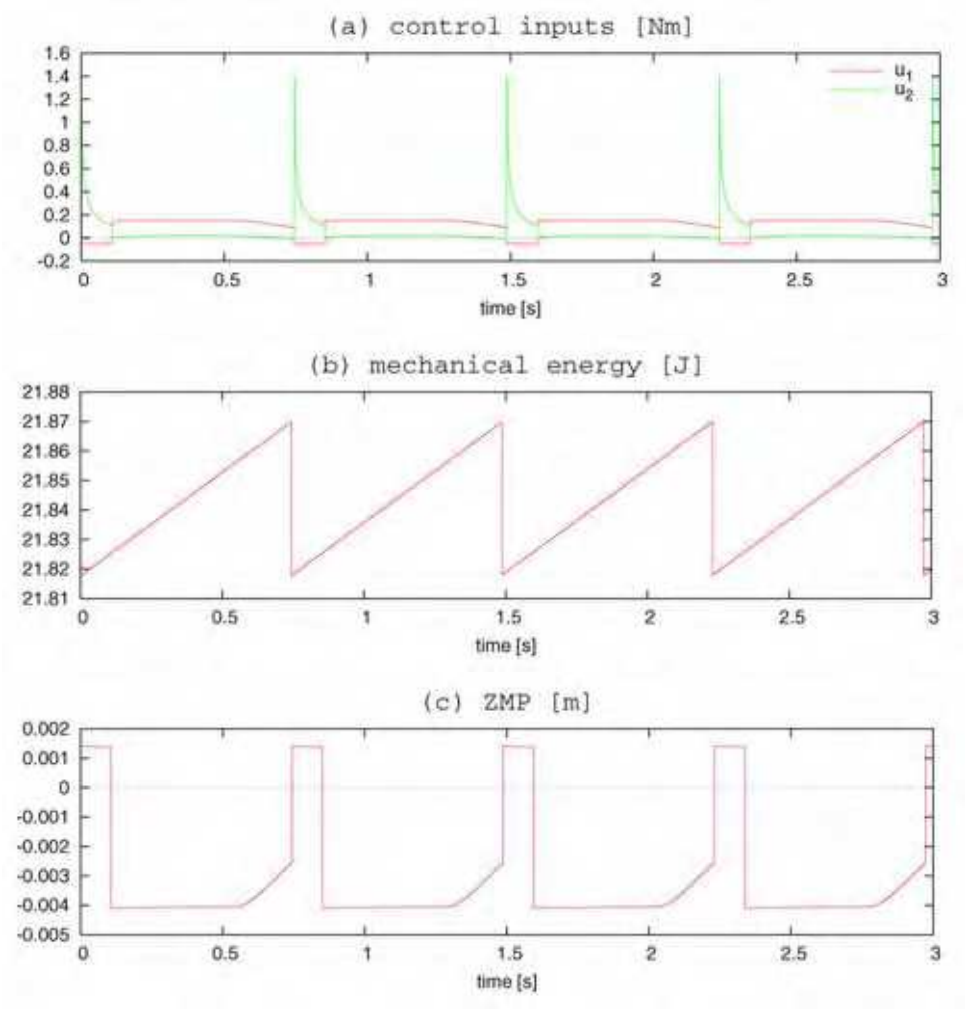

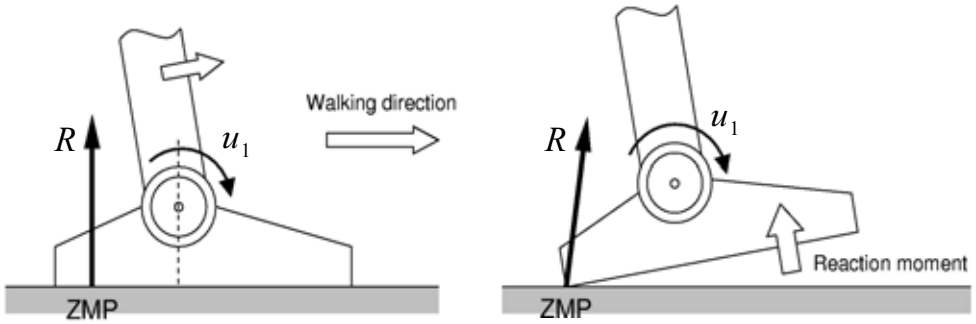

Fig. 5. Simulation results of dynamic walking by ECC considering ZMP control.

4.5 Switching Control

In order to manipulate the ZMP as well as to avoid the singularity, we must consider a switching algorithm from the principal ankle to hip-joint torque control. We here introduce the switching timing as $\theta_1 = \psi$ [rad]. At this instant, we reset η so that u_2 becomes continuous according to the following relationship:

$$u_2 = \eta\left(\dot{\theta}_1^{\mathrm{sw}} - \dot{\theta}_2^{\mathrm{sw}}\right) = \frac{\lambda - \dot{\theta}_1^{\mathrm{sw}} u^+}{\dot{\theta}_1^{\mathrm{sw}} - \dot{\theta}_2^{\mathrm{sw}}}. \tag{24}$$

from which we can calculate η as follows:

$$\eta = \frac{\lambda - \dot{\theta}_1^{\mathrm{sw}} u^+}{\left(\dot{\theta}_1^{\mathrm{sw}} - \dot{\theta}_2^{\mathrm{sw}}\right)^2} \tag{25}$$

where the superscript "sw" stands for the *switching* instant. The obtained η is used during its cycle and reset at every switching instant. Since u_2 is continuous, u_1 also becomes continuous.

Fig. 5 shows the simulation results of the dynamic walking by ECC with the proposed switching control. The control parameters are chosen as $\lambda = 0.07$ [J/s], $u^+ = 0.15$, $u^- = -0.05$ [Nm] and $\psi = 0.05$ [rad], respectively. By the effect of the principal ankle –joint torque control, the ZMP is shifted forward the ankle-joint without destroying the energy restoration condition. From Fig. 5 (b), we can see that the hip-joint torque becomes very large during the ZMP is shifted forward, but this does not affect the ZMP condition and the postural stability of foot is maintained.

4.6 Discussion

Here, we compare our method with approach proposed by Goswami *et al.* "energy tracking control." (Goswami *et al.*, 1997) Their approach is formulated as

$$\dot{E} = -\lambda_{\mathrm{etc}}\left(E - E^*\right), \tag{26}$$

where E^* [J] (constant) is the reference energy and positive scalar λ_{etc} is the feedback gain. A solution of Eq. (13) by constant torque ratio $\mu > 0$ which gives the condition $u_1 = \mu u_2$ is obtained as

$$\boldsymbol{\tau} = \frac{-\lambda_{\text{etc}}\left(E - E^*\right)}{\left(\mu+1\right)\dot{\theta}_1 - \dot{\theta}_2}\begin{bmatrix}\mu+1\\ -1\end{bmatrix}, \tag{27}$$

and in our case, a solution by constant torque ratio is given by

$$\boldsymbol{\tau} = \frac{\lambda}{\left(\mu+1\right)\dot{\theta}_1 - \dot{\theta}_2}\begin{bmatrix}\mu+1\\ -1\end{bmatrix}. \tag{28}$$

Figs. 6 and 7 respectively show the simulation results of active dynamic walking on a level by the torques of Eqs. (27) and (28) without manipulating the ZMP actively. The two cases are equal in walking speed. From the simulation results, we can see that, in our approach, the maximum ankle-joint torque is about 3 times smaller than that of Goswami's approach and this yields better ZMP condition. In this sense, we should conclude that the mechanical energy must be restored efficiently but its time-change rate should be carefully chosen to guarantee the ZMP condition.

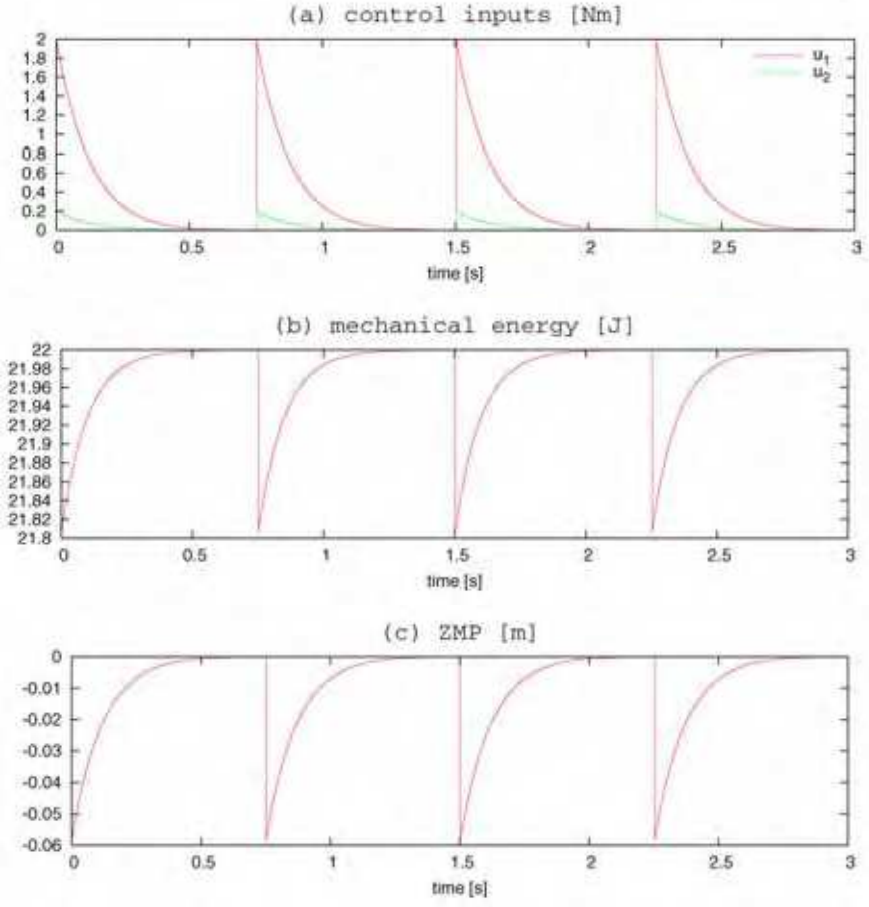

Fig. 6. Simulation results of dynamic walking by energy tracking control where $\lambda_{\text{etc}} = 10.0$, $\mu = 10.0$ and $E^* = 22.0$ [J].

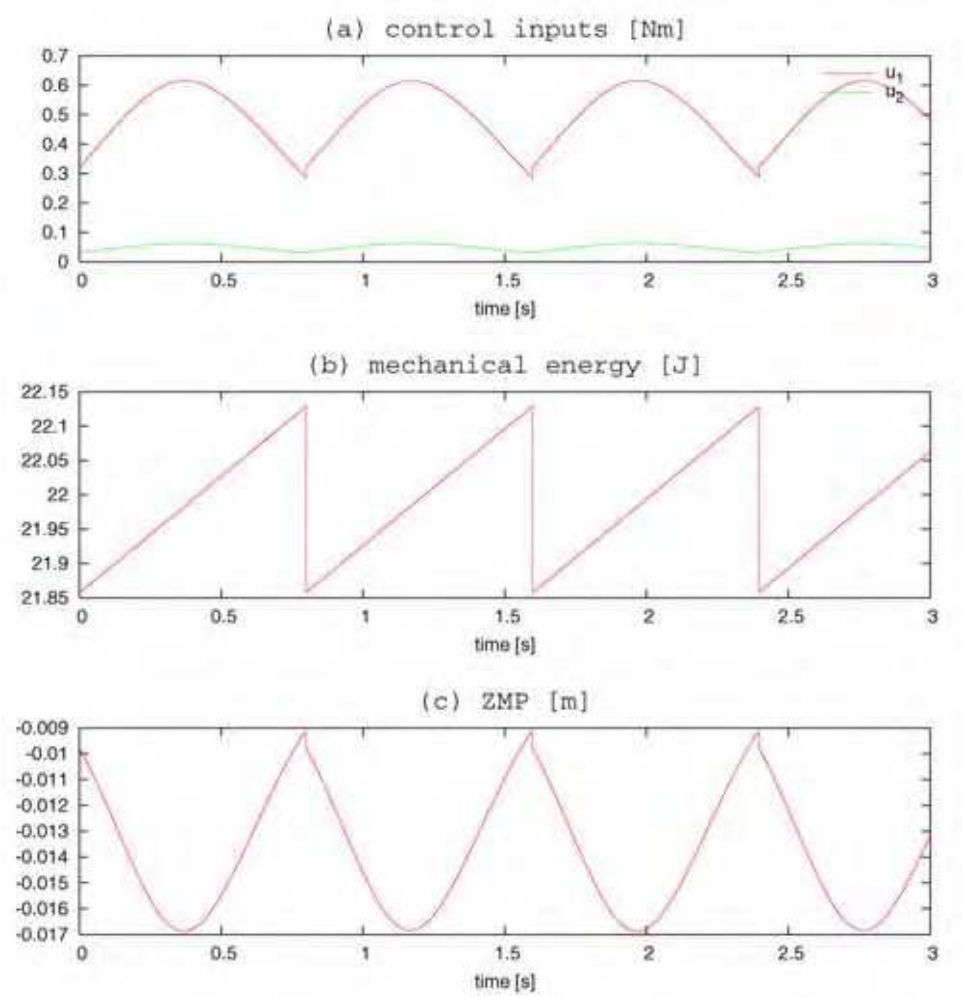

Fig. 7. Simulation results of dynamic walking by ECC where $\lambda = 0.34$ [J/s] and $\mu = 10.0$.

5. Experiments

In order to confirm the validity of the proposed method, we carried out actual walking experiment using our developed machine introduced in Fig.1. All encoders of the servomotors are interfaced to a computer (Pentium III 1.0 GHz) running Windows 98. To implement the control law, we used RtMaTX (Koga, 2000) for real-time computation with the sampling period 1.0 [ms].

Since the proposed methods are so called *model-matching control*, they are not robust for uncertainty. In this research, we use model following control of the motion generated by VIM (Virtual Internal Model) which is a reference model in computer. Every post-impact condition of VIM is reset to that of the actual machine. By using the VIM, the uncertainties

of identification, which is crucial factor in the case of model matching control, can be compensated. The dynamics of VIM is given by

$$\hat{\boldsymbol{M}}(\boldsymbol{\theta}_{\mathrm{d}})\ddot{\boldsymbol{\theta}}_{\mathrm{d}} + \hat{\boldsymbol{C}}(\boldsymbol{\theta}_{\mathrm{d}}, \dot{\boldsymbol{\theta}}_{\mathrm{d}})\dot{\boldsymbol{\theta}}_{\mathrm{d}} + \hat{\boldsymbol{g}}(\boldsymbol{\theta}_{\mathrm{d}}) = \boldsymbol{\tau}_{\mathrm{d}}, \tag{29}$$

where $\boldsymbol{\tau}_{\mathrm{d}}$ is the control input to drive the VIM and is determined by $\boldsymbol{\theta}_{\mathrm{d}}$ and $\dot{\boldsymbol{\theta}}_{\mathrm{d}}$. The control input for the actual robot is given by

$$\begin{aligned} \boldsymbol{\tau} &= \hat{\boldsymbol{M}}(\boldsymbol{\theta}_{\mathrm{d}})\boldsymbol{u} + \hat{\boldsymbol{C}}(\boldsymbol{\theta}_{\mathrm{d}}, \dot{\boldsymbol{\theta}}_{\mathrm{d}})\dot{\boldsymbol{\theta}}_{\mathrm{d}} + \hat{\boldsymbol{g}}(\boldsymbol{\theta}_{\mathrm{d}}) \\ \boldsymbol{u} &= \ddot{\boldsymbol{\theta}}_{\mathrm{d}} + \boldsymbol{K}_D\left(\dot{\boldsymbol{\theta}}_{\mathrm{d}} - \dot{\boldsymbol{\theta}}\right) + \boldsymbol{K}_P\left(\boldsymbol{\theta}_{\mathrm{d}} - \boldsymbol{\theta}\right) + \boldsymbol{K}_I \int\left(\boldsymbol{\theta}_{\mathrm{d}} - \boldsymbol{\theta}\right)\mathrm{d}t \end{aligned} \tag{30}$$

The virtual internal model started walking from the following initial condition:

$$\dot{\boldsymbol{\theta}}(0) = \begin{bmatrix} 0.68 \\ 0.62 \end{bmatrix}, \boldsymbol{\theta}(0) = \begin{bmatrix} -0.14 \\ 0.14 \end{bmatrix},$$

and its state was calculated and updated in real-time. At every transition instant, the angular positions of VIM were reset to that of the actual machine. PID controller drives the ankle-joint of the swing leg during the single-support phase so that the foot keeps the posture horizontal.

The experimental results are shown in Fig. 8. The adjustment parameters are chosen as $\lambda = 0.075$ [J/s], $u^{+} = 0.15$, $u^{-} = -0.05$ [Nm] and $\psi = 0.05$ [rad] empirically. Fig. 8 (a) and (b) show the evolution of angular positions and velocities of the actual machine, respectively. The actual angular velocities are calculated by differentiation thorough a filter whose transfer function is $70/(s+70)$. A stable dynamic walking is experimentally realized based on ECC via model following control.

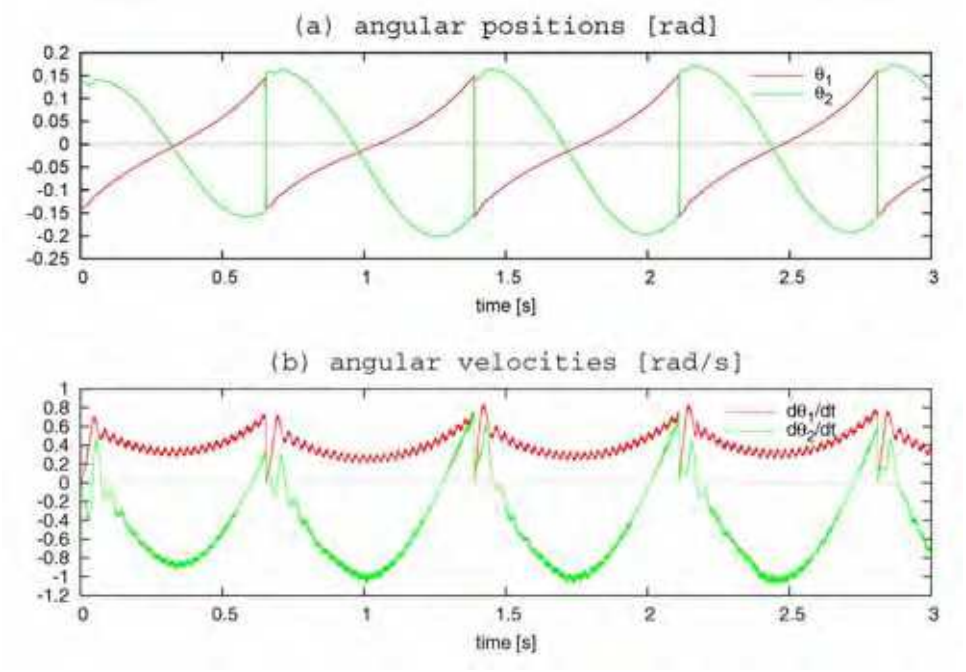

Fig. 8. Experimental results of dynamic walking by ECC.

6. Improving Robust Stability by Energy Feedback Control

Eq. (26) implies that the walking system becomes robust through the reference energy tracking. In other words, this control expands the basin of attraction of a limit cycle, however, our method Eq. (13) is so called the *feed-forward* control, which gives only energy change ratio without any information to attract the trajectories. Based on the observations, in this section, we firstly analyze the stability of the walking cycle and then consider an energy feedback control law in order to increase the robustness of the walking system.

Let us then consider an energy feedback control using a reference energy trajectory. Consider the following control

$$\dot{E} = \dot{\boldsymbol{\theta}}^{\mathrm{T}} \boldsymbol{S}\boldsymbol{u} = \dot{E}_{\mathrm{d}} - \zeta\left(E - E_{\mathrm{d}}\right), \tag{31}$$

which determines the control input so that the closed energy system yields

$$\frac{\mathrm{d}}{\mathrm{d}t}\left(E - E_{\mathrm{d}}\right) = -\zeta\left(E - E_{\mathrm{d}}\right) \tag{32}$$

where $\zeta > 0$ is the feedback gain. The original energy constraint control can be recognized as the case of $\dot{E}_{\mathrm{d}} = \lambda$ and $\zeta = 0$ in Eq. (31). By integrating Eq. (11) w.r.t. time, we can obtain the reference energy E_{d} using virtual time s as

$$E_{\mathrm{d}}(s) = E_0 + \lambda s \tag{33}$$

where E_0 [J] is the energy value when $s = 0$ [s]. A solution of Eq. (31) using constant torque ratio μ yields

$$\boldsymbol{S}\boldsymbol{u} = \frac{\dot{E}_{\mathrm{d}} - \zeta\left(E - E_{\mathrm{d}}\right)}{\left(\mu + 1\right)\dot{\theta}_1 - \dot{\theta}_2}\begin{bmatrix} \mu + 1 \\ -1 \end{bmatrix}. \tag{34}$$

Although *autonomy* of the walking system is destroyed by this method, we can improve the robustness of the walking system.

One way to examine the gait stability is Poincaré return map from a heel-strike collision to the next one. The Poincaré return map is denoted below as $\boldsymbol{F}$:

$$\boldsymbol{x}_{k+1} = \boldsymbol{F}\left(\boldsymbol{x}_k\right) \tag{35}$$

where the discrete state $\boldsymbol{x}_k$ is chosen as

$$\boldsymbol{x}_k = \begin{bmatrix} \theta_2^+[k] - \theta_1^+[k] \\ \dot{\theta}_1^+[k] \\ \dot{\theta}_2^+[k] \end{bmatrix}, \tag{36}$$

that is, relative hip joint angle and angular velocities just after k-th impact. The function $\boldsymbol{F}$ is determined based on Eqs. (1) and (3), but cannot be expressed analytically. Therefore, we must compute $\boldsymbol{F}$ by numerical simulation following an approximation algorithm.

In the case of steady walking, the relation $\boldsymbol{F}\left(\boldsymbol{x}^*\right) = \boldsymbol{x}^*$ holds and $\boldsymbol{x}^*$ is the equilibrium point of state at just after transition instant. For a small perturbation $\delta\boldsymbol{x}_k$ around the limit cycle, the mapping function $\boldsymbol{F}$ can be expressed in terms of Taylor series expansion as

$$\boldsymbol{F}\left(\boldsymbol{x}_k\right) = \boldsymbol{F}\left(\boldsymbol{x}^* + \delta\boldsymbol{x}_k\right) \approx \boldsymbol{x}^* + \nabla\boldsymbol{F} \cdot \delta\boldsymbol{x}_k \tag{37}$$

where

$$\nabla F \triangleq \frac{\partial F(x)}{\partial x}\bigg|_{x=x*} \tag{38}$$

is the Jacobian (gradient) around $\boldsymbol{x}^*$. By performing numerical simulations, $\nabla \boldsymbol{F}$ can be calculated approximately. The all eigenvalues of $\nabla \boldsymbol{F}$ are in the unit circle and the results are omitted. Although the robustness of the walking system is difficult to evaluate mathematically, the maximum singular value of $\nabla \boldsymbol{F}$ should imply the convergence speed of gait; smaller the value is, faster the convergence to the steady gait is. Fig. 9 shows the analysis result of maximum singular value of $\nabla \boldsymbol{F}$ w.r.t ζ in the Fig. 7 case with energy feedback control where $E_0 = 21.8575$ [J] and $\zeta = 10.0$. The maximum singular value monotonically decreases with the increase of ζ. The effect of improvement of the gait robustness by feedback control can be confirmed. Although applying this method destroys autonomy of the walking system, we can improve the robustness.

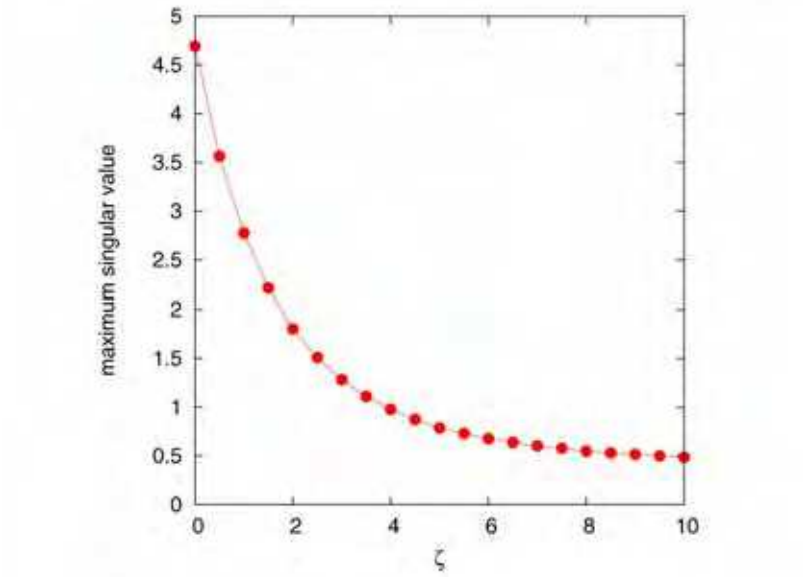

Fig. 9. Maximum singular value of $\nabla \boldsymbol{F}$ w.r.t. the feedback gain ζ.

6. Extension to a Kneed Biped

This section considers an extension of ECC to a kneed biped model. We treat a simple planar kneed biped model shown in Fig. 10, and its dynamic equation is given by

$$\boldsymbol{M}(\boldsymbol{\theta})\ddot{\boldsymbol{\theta}} + \boldsymbol{C}(\boldsymbol{\theta}, \dot{\boldsymbol{\theta}})\dot{\boldsymbol{\theta}} + \boldsymbol{g}(\boldsymbol{\theta}) = \boldsymbol{S}\boldsymbol{u} = \begin{bmatrix} 1 & 1 \\ 0 & -1 \\ 0 & 0 \end{bmatrix} \begin{bmatrix} u_1 \\ u_2 \end{bmatrix} \tag{39}$$

We consider the following assumptions.

1. The knee-joint is passive.
2. It can be mechanically locked-on and off.

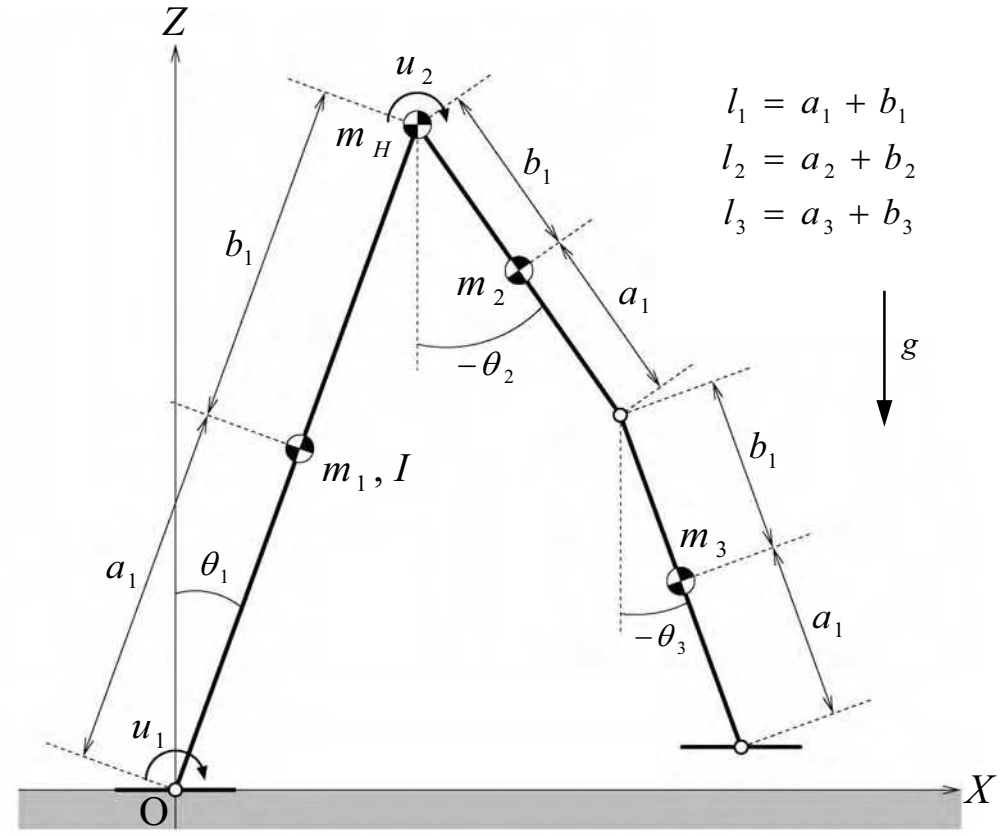

Fig. 10. Model of a planar underactuated biped robot.

The ECC then yields a problem of how to solve the following redundant equation:

$$\dot{E} = \dot{\theta}_1 u_1 + \left(\dot{\theta}_1 - \dot{\theta}_2\right) u_2 = \lambda \tag{40}$$

for the control inputs in real-time. Since the knee-joint is free, we can give the control input by applying the form of Eq. (28) as

$$\boldsymbol{Su} = \begin{bmatrix} \dfrac{\lambda}{(\mu+1)\dot{\theta}_1 - \dot{\theta}_2} \begin{bmatrix} \mu+1 \\ -1 \end{bmatrix} \\ 0 \end{bmatrix}. \tag{40}$$

On the other hand, a kneed biped has a property of obstacle avoidance, in other words, guaranteeing the foot clearance by knee-bending. To improve the advantageous, we introduce an active knee-lock algorithm proposed in our previous work (Asano & Yamakita, 2001) in the following. The passive knee-strike occurs when $\theta_2 = \theta_3$ during the single-support phase, and its inelastic collision model is given by

$$\boldsymbol{M}(\boldsymbol{\theta})\dot{\boldsymbol{\theta}}^{+} = \boldsymbol{M}(\boldsymbol{\theta})\dot{\boldsymbol{\theta}}^{-} - \boldsymbol{J}_I^{\mathrm{T}}\lambda_I \tag{41}$$

where $\boldsymbol{J}_I = [0 \quad 1 \quad -1]^{\mathrm{T}}$ and λ_I is the Lagrange's indeterminate multiplier vector and means the impact force. We introduce an active knee-lock algorithm before the impact and mechanically lock the knee-joint at a suitable timing. Let us then consider the dissipated mechanical energy at this instant. Define the dissipated energy ΔE_{ks} as

$$\Delta E_{ks} \triangleq \frac{1}{2}(\dot{\theta}^{+})^{\mathrm{T}} M(\theta)\dot{\theta}^{+} - \frac{1}{2}(\dot{\theta}^{-})^{\mathrm{T}} M(\theta)\dot{\theta}^{-} \leq 0 \tag{42}$$

This can be rearranged by solving Eq. (41) as

$$\Delta E_{\mathrm{ks}} = -\frac{1}{2}\left(\dot{\boldsymbol{\theta}}^{-}\right)^{\mathrm{T}} \boldsymbol{J}_I^{\mathrm{T}} \left(\boldsymbol{J}_I \boldsymbol{M}^{-1} \boldsymbol{J}_I^{\mathrm{T}}\right)^{-1} \boldsymbol{J}_I \dot{\boldsymbol{\theta}}^{-} = -\frac{\left(\dot{\theta}_2^{-} - \dot{\theta}_3^{-}\right)^2}{2\boldsymbol{J}_I \boldsymbol{M}^{-1} \boldsymbol{J}_I^{\mathrm{T}}} . \tag{43}$$

This shows that the condition to minimize the energy dissipation is $\dot{\theta}_2^{-} = \dot{\theta}_3^{-}$, and this leads $\Delta E_{\mathrm{ks}} = 0$. In general, there exists the timing in the kneed gait. After locking-on the knee-joint, we should lock-off it and the timing should be chosen empirically following a certain trigger. In this section, we consider the trigger as $X_g = 0$ [m] where X_g is the *X*-position of the robot's center of mass. Fig. 11 shows the phase sequence of a cycle with the knee-lock algorithm, which consists of the following phases.

1. Start
2. 3-link phase I
3. Active knee-lock on
4. Virtual compass phase (2-link mode)
5. Active knee-lock off
6. 3-link phase II
7. Passive knee-strike
8. Compass phase (2-link mode)
9. Heel-strike

Fig. 12 shows the simulation results of dynamic walking by ECC where $\lambda = 5.0$ and $\mu = 4.0$. The physical parameters are chosen as Table 2. From Fig. 12 (b) and (d), it is confirmed that the passive knee-joint is suitably locked-on without energy-loss, and after that, active lock-off and passive knee-strike occur. Fig. 13 shows the stick diagram for one step. We can see that a stable dynamic bipedal gait is generated by ECC.

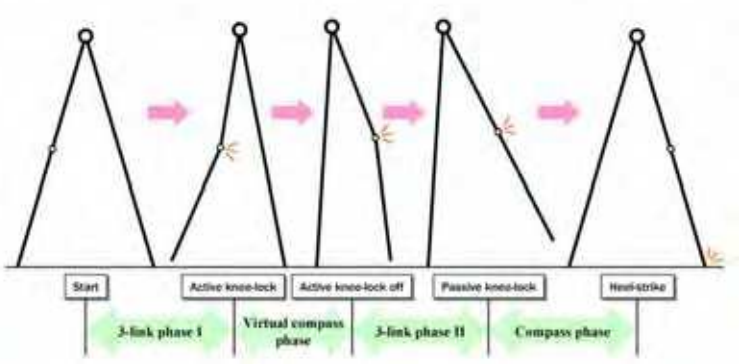

Fig. 11. Phase sequence of dynamic walking by ECC with active lock of free knee-joint.

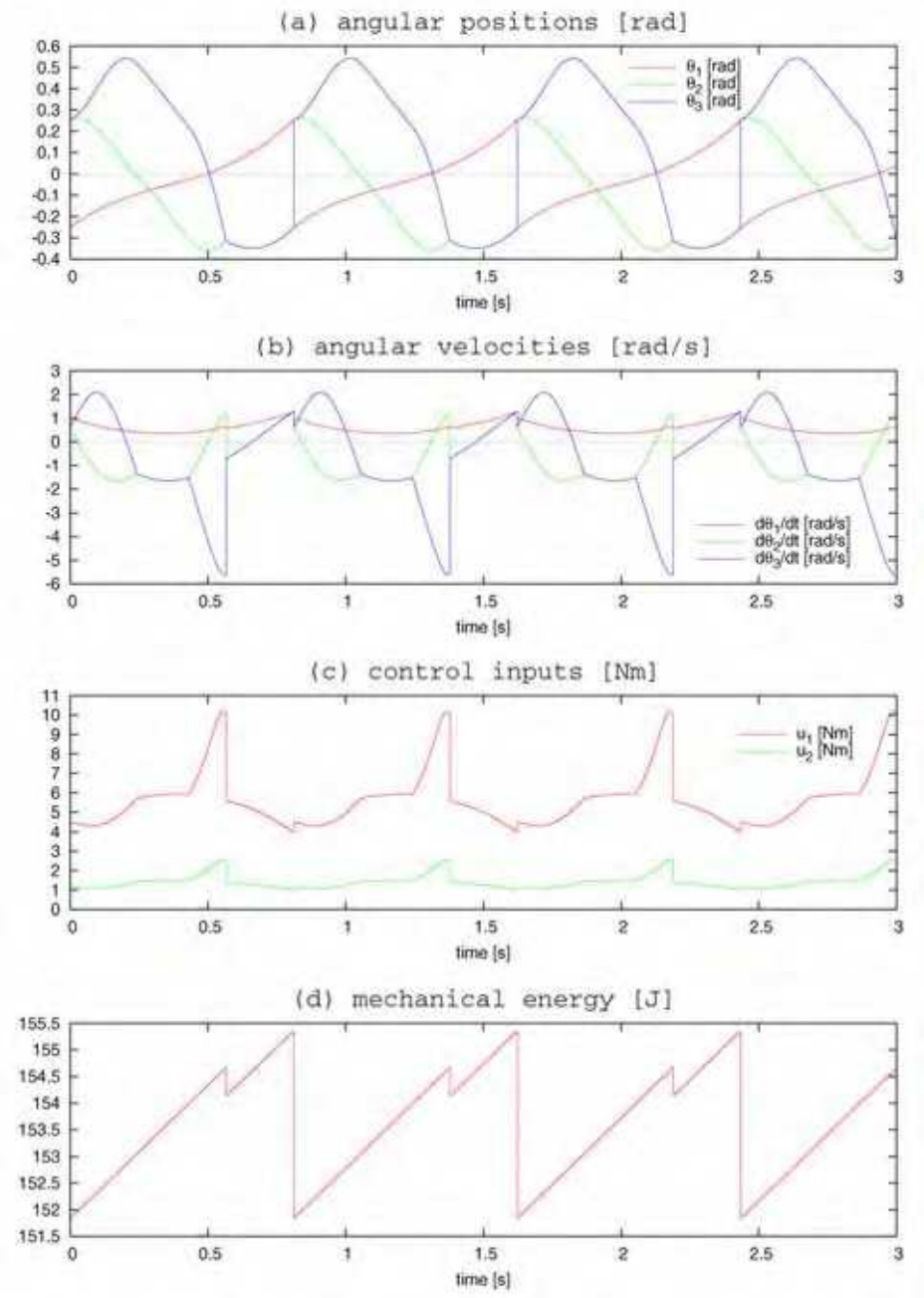

Fig. 12. Simulation results of dynamic walking of a kneed biped by ECC where $\lambda = 5.0$ [J/s] and $\mu = 4.0$.

m_1	$= m_2 + m_3$	5.0	kg
m_2		3.0	kg
m_3		2.0	kg
m_H		10.0	kg
I	$= m_2 m_3 \left(a_2 + b_3\right)^2 / m_1$	0.243	$\mathrm{kg \cdot m^2}$
a_1	$= \left(m_2 \left(l_3 + a_2\right) + m_3 a_3\right) / m_1$	0.52	m
b_1		0.48	m
a_2		0.20	m
b_2		0.30	m
a_3		0.25	m
b_3		0.25	m
l_1	$= a_1 + b_1$	1.00	m
l_2	$= a_2 + b_2$	0.50	m
l_3	$= a_3 + b_3$	0.50	m

Table 2. Parameters of the planar kneed biped.

Fig. 16. Stick diagram of dynamic walking with free knee-joint by ECC

7. Conclusions and Future Work

In this chapter, we have proposed a simple dynamic gait generation method imitating the property of passive dynamic walking. The control design technique used in this study was shown to be effective to generate a stable dynamic gait, and numerical simulations and experiments have proved its validity.

The authors believe that an energy restoration is the most essential necessary condition of dynamic walking and its concept is worth to be taken into consideration to generate a natural and energy-efficient gait. In the future, extensions of our method to high-dof humanoid robots should be investigated.

8. References

Asano, F. & Yamakita, M. (2001). Virtual gravity and coupling control for robotic gait synthesis, *IEEE Trans. on Systems, Man and Cybernetics Part A*, Vol. 31, No. 6, pp. 737-745, Nov. 2001.

Goswami, A.; Thuilot, B. & Espiau, B. (1996). Compass-like biped robot Part I: Stability and bifurcations of passive gaits, Research Report INRIA 2613, 1996.

Goswami, A.; Espiau, B. & Keramane, A. (1997). Limit cycles in a passive compass gait biped and passivity-mimicking control laws, *Autonomous Robots*, Vol. 4, No. 3, pp. 273-286, Sept. 1997.

Koga, M. (2000). Numerical Computation with MaTX (In Japanese), Tokyo Denki Univ. Press, ISBN4-501-53110-X, 2000.

McGeer, T. (1990). Passive dynamic walking, *Int. J. of Robotics Research*, Vol. 9, No. 2, pp. 62-82, April 1990.

Vukobuatović, M. & Stepanenko, Y. (1972). On the stability of anthropomorphic systems, Mathematical Biosciences, Vol. 15, pp. 1-37, 1972.

Humanoid Robots: New Developments

Edited by Armando Carlos de Pina Filho

ISBN 978-3-902613-00-4

Hard cover, 582 pages

Publisher I-Tech Education and Publishing

Published online 01, June, 2007

Published in print edition June, 2007

For many years, the human being has been trying, in all ways, to recreate the complex mechanisms that form the human body. Such task is extremely complicated and the results are not totally satisfactory. However, with increasing technological advances based on theoretical and experimental researches, man gets, in a way, to copy or to imitate some systems of the human body. These researches not only intended to create humanoid robots, great part of them constituting autonomous systems, but also, in some way, to offer a higher knowledge of the systems that form the human body, objectifying possible applications in the technology of rehabilitation of human beings, gathering in a whole studies related not only to Robotics, but also to Biomechanics, Biomimmetics, Cybernetics, among other areas. This book presents a series of researches inspired by this ideal, carried through by various researchers worldwide, looking for to analyze and to discuss diverse subjects related to humanoid robots. The presented contributions explore aspects about robotic hands, learning, language, vision and locomotion.

How to reference

In order to correctly reference this scholarly work, feel free to copy and paste the following:

Fumihiko Asano, Masaki Yamakita, Norihiro Kamamichi and Zhi-Wei Luo (2007). Biped Gait Generation and Control Based on Mechanical Energy Constraint, Humanoid Robots: New Developments, Armando Carlos de Pina Filho (Ed.), ISBN: 978-3-902613-00-4, InTech, Available from: http://www.intechopen.com/books/humanoid_robots_new_developments/biped_gait_generation_and_control_based_on_mechanical_energy_constraint

INTECH
open science | open minds

InTech Europe
University Campus STeP Ri
Slavka Krautzeka 83/A
51000 Rijeka, Croatia
Phone: +385 (51) 770 447
Fax: +385 (51) 686 166
www.intechopen.com

InTech China
Unit 405, Office Block, Hotel Equatorial Shanghai
No.65, Yan An Road (West), Shanghai, 200040, China
中国上海市延安西路65号上海国际贵都大饭店办公楼405单元
Phone: +86-21-62489820
Fax: +86-21-62489821